The firn meltwater Retention Model Intercomparison Project (RetMIP): Evaluation of nine firn models at four weather station sites on the Greenland ice sheet

Baptiste Vandecrux[1,2], Ruth Mottram[3], Peter L. Langen[3], Robert S. Fausto[1], Martin Olesen[3], C. Max Stevens[4], Vincent Verjans[5], Amber Leeson[5], Stefan Ligtenberg[6], Peter Kuipers Munneke[6], Sergey Marchenko[7], Ward van Pelt[7], Colin Meyer[8], Sebastian B. Simonsen[9], Achim Heilig[10], Samira Samimi[11], Horst Machguth[12], Michael MacFerrin[13], Masashi Niwano[14], Olivia Miller[15], Clifford I. Voss[16], Jason E. Box[1]

[1] Geological Survey of Denmark and Greenland, Copenhagen, Denmark.
[2] Department of Civil Engineering, Technical University of Denmark, Lyngby, Denmark.
[3] Danish Meteorological Institute, Copenhagen, Denmark
[4] Department of Earth and Space Sciences, University of Washington, WA USA
[5] Lancaster Environment Centre, Lancaster University, Lancaster, UK
[6] IMAU, Utrecht University, The Netherlands
[7] Department of Earth Sciences, Uppsala University, Uppsala, Sweden
[8] Thayer School of Engineering, Dartmouth College
[9] National Space Institute, Technical University of Denmark, Kgs. Lyngby, Denmark
[10] Department of Earth and Environmental Sciences, LMU, Munich, Germany
[11] Department of Geography, University of Calgary, Calgary, AB, Canada
[12] Department of Geosciences, University of Fribourg, Switzerland
[13] Cooperative Institute for Research in Environmental Sciences, University of Colorado, Boulder, CO, USA
[14] Meteorological Research Institute, Japan Meteorological Agency, Tsukuba, 305-0052 Japan
[15] U. S. Geological Survey, Utah Water Science Center, Salt Lake City, UT, USA
[16] U. S. Geological Survey, Menlo Park, CA, USA

Correspondence to: B. Vandecrux (bav@geus.dk)

Abstract. Perennial snow, or firn, covers 80% of the Greenland ice sheet and has the capacity to retain part of the surface meltwater, buffering the ice sheet's contribution to sea level. Multi-layer firn models are traditionally used to simulate the firn processes and estimate meltwater retention. We present the output from nine firn models, forced by weather-station-derived mass and energy fluxes at four sites representative of the dry snow, percolation, ice slab and firn aquifer areas. We compare the model outputs and evaluate them against in situ observations. Models that explicitly account for deep meltwater percolation overestimate percolation depth and consequently firn temperature at the percolation and ice slab sites although they accurately simulate the recharge of the firn aquifer. Models using Darcy's law and a bucket scheme compare favourably to observations at the percolation site but only the Darcy models accurately simulate firn temperature and thus meltwater percolation at the ice slab site. We find that Eulerian models, that transfer firn through fixed layers, smooth sharp gradients in firn temperature and density over time. From the model spread, we find that simulated densities (respectively temperature)

The Cryosphere
Discussions

EGU Open Access

have an uncertainty envelope of ± 60 kg m^{-3} (resp. ± 14 ºC) in the dry snow area and up to ± 280 kg m^{-3} (resp. ± 15-18 ºC) at warmer sites.

40 **1. Introduction**

Responding to higher air temperatures and increased surface melt, the Greenland ice sheet has been losing mass at an accelerating rate over the last decades and is responsible for about 20% of the current global sea level rise (Van den Broeke et al. 2016, IMBIE Team 2019). The temperature increase has introduced melt at higher elevations, where melt was seldomly seen (Nghiem et al. 2012). In these colder, elevated areas, snow builds up into a thick layer of firn. Increased surface melt in

45 the firn area of the Greenland ice sheet was seen to affect the firn structure (Machguth et al. 2016; Mikkelsen et al. 2015), density (De La Peña et al. 2015; Vandecrux et al. 2018), air content (van Angelen et al. 2013; Vandecrux et al. 2019) and temperature (Polashenski et al. 2014; Van den Broeke et al., 2016). Changing firn characteristics affect how much meltwater can be refrozen within the firn (Braithwaite et al., 1994; Pfeffer et al., 1991) or retained as long-term liquid water storage in perennial firn aquifers (e.g. Forster et al. 2014; Miège et al. 2016)   and therefore the ice-sheet contribution to sea-level rise

50 (Harper et al., 2012; Machguth et al. 2016; Mikkelsen et al. 2015; Van As et al. 2017). Meltwater refreezing can saturate the firn, forming continuous ice layers of several meters in thickness (MacFerrin et al. 2019). These ice slabs impede meltwater percolation of meltwater, enhance meltwater runoff, and lower the surface albedo (Charalampidis et al. 2015) further amplifying Greenland's contribution to sea-level rise. The firn on the Greenland ice sheet has been investigated for two additional reasons. First, knowledge about how firn air content evolves through time is necessary for the conversion of space-

55 borne observations of ice sheet volume change into mass change (e.g. Simonsen et al. 2013; Sørensen et al. 2011). Secondly, the depth of firn to ice transition as well as the mobility of gases through the firn before they are trapped in bubbles within glacial ice are necessary for the interpretation of ice cores and heavily depend on the fine coupling between the firn characteristics and the surface conditions (Spencer et al., 2001; Goujon et al., 2003).

60 Snow and firn models have been coupled to regional climate models to describe the evolution of firn characteristics and meltwater retention. However, various models have been used, all using differing formulations and numerical strategies to describe the firn processes. Earlier, Reijmer at al. (2012) showed that, provided reasonable tuning, simple parameterizations of the subsurface processes return similar refreezing rates for the Greenland ice sheet, which were also in agreement with the results from two physically based layered subsurface models. However, the spatial patterns varied widely and validation

65 against field observations remained challenging. The meltwater Retention Model Intercomparison Project (RetMIP) aims at comparing some of the models currently used on the Greenland ice sheet coordinated by using the same surface inputs of mass and energy for all participating firn models. In this publication, we evaluate nine firn models at four sites where surface conditions could be derived from automatic weather station observations and where firn observations are available.

70   We here aim to answer the following questions: What is the model-induced variability in simulated firn density, temperature and liquid water content? What is the impact of model design on the output and what are the uncertainties that apply to the firn models' outputs? We address these questions at four sites that are representative of different firn regimes: a dry snow site, a site in the percolation area, an ice slabs site and lastly a firn aquifer location. At each site, the models are forced by weather-station-derived mass and energy fluxes and initialized with observed profiles of firn temperature and density. The model

75   outputs are thereafter compared to observations of firn density, temperature, percolation depth and their variability, performance and uncertainties are discussed.

2.   Models

The multi-layer firn models investigated here are listed in Table 1 and all have density, temperature, and liquid water content as prognostic variables. They all follow the general framework: they divide the firn into multiple layers for which firn

80   characteristics can be calculated. The number of layers vary in each model (Table 2) and we distinguish between two distinct types of layer management strategies: All models except DMIHH and MeyerHewitt follow a Lagrangian framework: they add new layers at the top of the model column during snowfall and these layers are advected downward as new material accumulates at the surface. DMIHH and MeyerHewitt follow a Eulerian framework in which the layers have either fixed mass or fixed volumes. During snowfall, new material is added to the first layer and an equivalent mass/volume is transferred by

85   each layer to the underlying neighbour. At each time step, the models calculate firn density according to various densification laws and update the layer temperature using different values of thermal conductivity (Table 2). The DMIHH, GEUS and DTU models have a fixed temperature at the bottom of their column (Dirichlet boundary condition) while other models have fixed temperature gradient (Neuman boundary condition). All models simulate meltwater percolation and transfer water from one layer to the next according to the routines listed in Table 2, as well as meltwater refreezing and latent heat release. All models

90   simulate the retention of meltwater within a layer due to capillary suction, either explicitly (MeyerHewitt and CFM model) or, for all other models, through the use of an irreducible water content as parameterised by Coléou and Lesaffre (1991). When meltwater cannot be transferred to the next layer or be retained within the layer by capillary suction, lateral runoff can occur according to certain rules depending on the model (Table 2). The models background and specificities are described in greater detail in the following paragraphs.

95

Table 1: Models evaluated in this study.

Model code name	Developing institute	References
CFM-Cr **CFM-KM**	University of Washington, University of Lancaster	Stevens et al. (2020) Verjans et al. (2019)
DTU	Technical University of Denmark – National Space Institute	Sørensen et al. (2011); Simonsen et al. (2013)
DMIHH	Danish Meteorological Institute	Langen et al. (2017)
GEUS	Geological Survey of Denmark and Greenland	Vandecrux et al. (2018)
IMAU-FDM	Institute for Marine and Atmospheric research Utrecht (IMAU), Utrecht University	Ligtenberg et al. (2011), Kuipers Munneke et al. (2015; Ligtenberg et al. (2018)
MeyerHewitt	Thayer School of Engineering, Dartmouth College	Meyer and Hewitt (2017)
UppsalaUniBucket **UppsalaUniDeepPerc**	Uppsala University	Van Pelt et al. (2012) Marchenko et al. (2017) Van Pelt et al. (2019)

2.1. CFM-Cr and CFM-KM

The Community Firn Model (CFM) is an open-source, modular model framework designed to simulate numerous physical processes in firn (Stevens, 2018). The number of layers is not fixed; new snow accumulation at each time step is added as a new layer, and a layer-merging routine prevents the number of layers from becoming too large. The CFM-Cr and CFM-KM use different densification scheme (Table 2) and the same meltwater percolation scheme: a dual-domain approach that closely follows the implementation of the SNOWPACK snow model (Wever et al. 2016). It accounts for the duality of water flow in firn by simulating both slow matrix flow and fast, localised, preferential flow after Verjans et al. (2019). In the matrix flow domain, water percolation is prescribed by the Richards Equation, ice layers are impermeable, and runoff is allowed. In contrast, preferential flow can bypass such barriers and no runoff is simulated. Water is exchanged between both domains as a function of the firn layer properties: density, temperature and grain size. As such, when water in the matrix flow domain

accumulates above an ice layer, it is progressively depleted by runoff and by transfer of water in the preferential flow domain. In the deepest firn layers, above the impermeable ice-sheet, water accumulates, and no runoff is prescribed, which allows for the build-up of firn aquifers.

2.2. DTU

The DTU firn model was developed to aid the interpretation of elevation change observations from NASA's ICESat satellite altimeter mission in relation to deriving the Greenland ice sheet mass balance (Sørensen et al., 2011). Further, the DTU model development was targeted at modelling the inter-annual stratigraphy of the dry-snow zone along the EGIG-line in central Greenland as mapped by the ASIRAS-instrument, an airborne version of the ESAs CRYOSat-2 satellite altimeter mission. The DTU model is founded in the empirical frame of the HL-model as modified by Arthern et al. (2010). The model is a 1D column model which includes the formation of ice lenses following the formulation by Reeh (2005). Meltwater retention follows the bucket approach to distribute rain or meltwater from the surface. If meltwater is conveyed to a model layer, the water is refrozen if there are sufficient pore space and cold content available in the layer. Additional liquid water can be retained in a layer by capillary forces (Schneider and Jansson 2004). This formulation does not allow for the formation of firn aquifers. Percolation continues until the water encounters a layer at ice density or the bottom of the model where, in both cases, it is assumed to run off. The model follows a Lagrangian scheme of advection of layers down into the firn and the model layering is defined by the time-stepping of the model. Model layers may be empty if no precipitation is received at the surface a given time step or if the surface layer is melted away by meltwater production ascribed by the forcing.

2.3. DMIHH

The DMIHH model was developed to provide firn subsurface details for the HIRHAM regional climate model experiments (Langen et al., 2017). DMIHH employs 32 layers of time-constant water equivalent thicknesses divided into contributions from snow, ice and liquid water. Layer thicknesses increase with depth to increase resolution near the surface and give a full model depth of 60 m w.e.. Mass added at the surface (e.g., snowfall) or removed as runoff causes the scheme to advect mass downward or upward to ensure the constant w.e. layer thicknesses. In addition to the saturated and unsaturated hydraulic conductivities (Table 2), the water flow through layers containing ice follows the analytical model of Colbeck (1975) for a snowpack with interspersed ice layers. A parameter describing the ratio between the width of holes in the ice and the width of the ice must be chosen and we choose here a value of 1, meaning that ice has a horizontal extent of half the unit area. A layer is considered impermeable if its bulk dry density exceeds $810 \ kg \ m^{-3}$. Runoff is calculated from the water in excess of the irreducible saturation with a characteristic local runoff time-scale that increases as the surface slope tends to zero (Zuo and Oerlemans, 1996), with the coefficients of the time-scale parameterization from Lefebre et al. (2003). DMIHH has an

initial value of 0.1 mm for the grain diameter of freshly fallen snow. The column grain size distribution is initialized in these experiments as columns taken at the specific sites from the spinup experiments performed by Langen et al. (2017).

140 **2.4. GEUS**

The GEUS model is based on the DMIHH model (Langen et al., 2017) and is further developed in Vandecrux et al. (2018, in review). As in the DMIHH model, the layer's ice content decreases its hydraulic conductivity according to Colbeck (1974) but we set the geometry parameter to 0.1 as detailed in Vandecrux et al. (2018). At the end of a time step, water exceeding the irreducible water content that could not be percolated downward is assumed to runoff and removed from the layer at a rate

145 that depends on the firn characteristics and on surface slope according to Darcy's law. See more details about this runoff scheme in the Supplementary text S1.

2.5. IMAU-FDM

The IMAU-FDM model has been used in combination with the RACMO regional model in Greenland, on Arctic Canada and Antarctica. Firn compaction follows a semi-empirical, temperature-based equation from Arthern (2010). The compaction rate

150 is tuned to observations from Greenland firn cores using an accumulation-based correction factor (Kuipers Munneke et al., 2015). IMAU-FDM includes meltwater percolation following a tipping-bucket approach. Percolating meltwater is refrozen if there is space available in the layer, and if the latent heat of refreezing can be released in the layer. As opposed to other models in this study, runoff is not allowed over ice layers, but only when percolating meltwater has reached the pore close-off depth. Upon reaching that depth, runoff is instantaneous. The rationale for allowing percolation through thick ice slabs is that IMAU-

155 FDM is mainly used to simulate firn at scales of tens to hundreds of square kilometres, and at these spatial scales, meltwater is assumed to always find a way through even the thickest of ice slabs.

2.6. MeyerHewitt

Meyer and Hewitt (2017) present a continuum model for meltwater percolation in compacting snow and firn. The MeyerHewitt model includes heat conduction, meltwater percolation and refreezing, as well as mechanical compaction using

160 the empirical Herron and Langway (1980) model. In the MeyerHewitt model, water percolation is described using Darcy's law, allowing for both partially and fully saturated pore space. Water is allowed to run off from the surface if the snow is fully saturated. Using an enthalpy formulation for the problem, the MeyerHewitt model is discretized using the conservative finite volume method that is fixed in the frame of the firn surface and is Eulerian, meaning that material can flow into and out of the domain.

165

Table 2: Model characteristics.

Model	Discretization	Meltwater routing	Hydraulic conductivity	Firn densification	Runoff calculation	Thermal conductivity
CFM-Cr	Unlimited number of layers. Lagrangian	Richards equation and dual-domain preferential flow scheme (Wever et al., 2016; Verjans et al., 2019)	van Genuchten (1980)	Vionnet et al. (2012)	Zuo and Oerlemans (1996)	Anderson (1976)
CFM-KM				Kuipers Munneke et al. (2015)		
DTU	Dynamically allocated, based on accumulation rates, timestep and depth range. Lagrangian	Bucket scheme	-	Sørensen et al. (2011); Simonsen et al. (2013)	Immediate runoff on top of an ice layer	Schwander et al. (1997)
GEUS	200 layers dynamically allocated, Lagrangian	Parameterization of Darcy's law	Calonne et al. (2012), Hirashima et al. (2010)	Vionnet et al. (2012)	Darcy flow to identical cell given surface slope	Calonne et al. (2011)
DMIHH	32 layers, Eulerian				Zuo and Oerlemans (1996)	Yen (1981)
IMAU-FDM	maximum of 3000 layers, Lagrangian	Bucket scheme	-	Kuipers Munneke et al. (2015)	Only at the bottom of the column	Anderson (1976)
MeyerHewitt	finite volume, Eulerian, 600 layers	Darcy's law	Carman-Kozeny	Herron and Langway (1980)	Excess surface water	constant
UppsalaUniBucket	600 layers, max 0.1 m layer thickness. Lagrangian	Bucket scheme	-	Ligtenberg et al. (2011)	Only at the bottom of the column	Sturm et al. (1997)
UppsalaUniDeepPerc		Deep percolation scheme; linear distribution down to 6 m (Marchenko et al. 2017)				

2.7. UppsalaUniBucket & UppsalaUniDeepPerc

UppsalaUniBucket and UppsalaUniDeepPerc have been developed for the Norwegian Arctic (Van Pelt et al. 2012; 2019; Marchenko et al., 2017) and only differ in their representation of vertical water transport. UppsalaUniBucket simulates melt
170 water percolation according to the tipping-bucket scheme while UppsalaUniDeepPerc uses a deep percolation scheme which mimics the effect of fast vertical transport due to preferential flow (Marchenko et al. 2017). The water transport model incorporates irreducible water storage but does not allow for standing water to accumulate on top of the impermeable ice;

instead all water that reaches the base of the firn column is set to runoff instantaneously. References for the parameterizations used for gravitational settling, thermal conductivity, irreducible water storage and water percolation are given in Table 2.

3. Methods

3.1. Forcing data

Differences between firn-model outputs and observations depend as much on the model formulation as on the forcing data that is given to the model (e.g., Ligtenberg et al., 2018). Any bias in forcing data propagates into the model output. To make sure we compare and evaluate the models independently of biases that may exist in forcing datasets that come from RCMs, we use meteorological fields derived from five weather stations at four sites. These sites represent a wide range of climatic conditions on the Greenland ice sheet (Table 4, Figure 1) that produce a wide variety of firn density and temperature profiles. For example, the cold and dry climate at Summit Station produces cold firn with low compaction rates representative of the "dry snow" area as defined by Benson (1962). Located in an area with higher melt (Table 3), Dye-2 is representative of the "percolation area" (Benson, 1962) where meltwater generated at the surface percolates into the firn and releases latent heat when refreezing into ice lenses. The Firn Aquifer (FA) site in Southeast Greenland, has both high surface melt and high accumulation rate, leading to the formation of a perennial body of liquid water at a depth of 20 m and below (Forster et al., 2012; Kuipers Munneke et al. 2014). At the KAN_U site, lower accumulation rates and increasing melt have led to the formation thick ice slabs (Machguth et al., 2016; MacFerrin et al., 2019) that impede meltwater percolation below 5 m.

We use data from GC-Net weather stations at Dye-2 and Summit (Steffen et al., 1996) from the PROMICE station at KAN_U (Ahlstrøm, et al., 2008; Charalampidis, et al., 2015), from IMAU, Utrecht University at the Firn Aquifer site (see Supplementary Text S2 for station description), and a weather station installed by Samira Samimi and Shawn Marshall at Dye-2 in 2016 (see Supplementary Text S2 for station description). The use of a different station at Dye-2 in 2016 (which was more recently installed than the GC-Net station), ensures the best meteorological forcing for the models over that melting season, during which an extensive validation dataset is available.
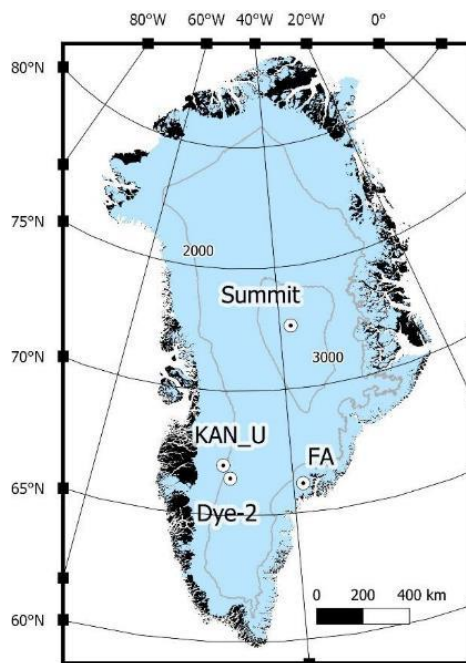
Figure 1: Map of the four study sites.

The data from each weather station are quality checked and obvious sensor malfunctions are discarded. The data availability after filtering of erroneous data at Summit, KAN_U and Dye-2_long is reported in Table S1. No data was discarded at FA

200 and Dye-2_16. The data gaps were filled using either nearby stations or HIRHAM5 data as in Vandecrux, et al. (2018). Downward longwave radiation is not monitored by the GC-Net stations (Dye-2 and Summit) and is taken entirely from HIRHAM5 output. The surface energy balance model developed by van As et al. (2005) was used as in Vandecrux et al. (2018) to calculate surface "skin" temperature, meltwater generation and net snow accumulation (precipitation – sublimation + deposition). These data averaged to three-hourly values were used to force all the firn models. When necessary, the given

205 input data were adapted to match the specific needs of certain firn models (see Supplementary Text S1). Rain is not monitored at any site, so it is not included in the mass fluxes. Tilt of the radiation sensor was not corrected for at Dye-2 and Summit stations although this correction was seen to increase the calculated melt by 35 mm w.e. yr^{-1} at Dye-2 (Vandecrux et al., in review). The surface forcing data is illustrated in Figure S1.

3.2. Boundary conditions

210 To allow comparison of the various firn models, as many boundary conditions as possible were given to all models. A key parameter to all firn models is the density of fresh snow when it is added at the top of the model column. Here, we use the value of 315 kg m^{-3} from Fausto et al. (2018) which is derived from a compilation of top 10 cm snow density observations from the Greenland ice sheet. The long-term accumulation and annual near-surface air temperature as well as the local surface

The Cryosphere
Discussions

215

Table 3: Information about the 5 sites considered in the pointwise model comparison.

Station name	Firn Aquifer (FA)	Summit	Dye-2_16	Dye-2_long	KAN_U
Elevation (m a.s.l.)	1563	3254	2165	2165	1840
Start date	12-04-2014	02-07-2000	02-05-2016	01-06-1998	01-05-2012
End date	02-12-2014	08-03-2015	28-10-2016	02-05-2015	31-12-2016
Mean annual accumulation (mm w.e.)	1739	159	476	476	543
Mean annual air temperature (°C)	-7	-26	-16	-16	-12.4
Surface slope (°)	0.6	0	0.2	0.2	0.5
Measured average deep firn temperature (°C)	0@25m	-31@10m	-13@9m	-15.5 @10 m	-9@5m
Initial firn density	Top 8 m: FA-14 (Montgomery et al., 2018) From 8 to 60 m: FA-13 (Koenig et al. 2014)	Top 8m: core from 1990 by Mayewski & Whitlow., (2016) From 8 to 60 m: GRIP core	Top 18 m: Core_10_2016 (B. Vandecrux et al. 2018) From 10 to 60 m: Dye-2 1998 core B (Mosley-Thompson, et al., 2001)	Dye-2 1998 core B (Mosley-Thompson et al. 2001)	Top 10 m: core_1_2012 (Machguth et al. 2016) From 10 to 60 m: Site J, 1989 (Kameda et al. 1995)

slope was prescribed according to Table 3. Initial profiles for density, temperature and liquid water content (only at FA) are

220 provided to all models and illustrated in Figure S2. The origin of the initial density profiles is given in Table 3. Initial temperature profiles were calculated using the first reading of air temperature (as first guess of surface temperature), the first valid measurement of firn temperature, and the deep firn temperature (Table 3). The deep firn temperature was calculated as the long-term mean at the deepest firn temperature measurement. Initial liquid water content at FA is calculated according to the observations from Koenig et al. (2014) indicating pore saturation below 12.2 m depth.

225 **3.3. Intercomparison and validation of model output**

Participating models provided firn density, temperature and liquid water content in 3 h time steps, interpolated to a common 10 cm grid from the surface to 20 m depth. Additionally, three-hourly vertically integrated refreezing and runoff were calculated by each model.

230 Three types of validation datasets are available at our sites: i) a set of firn-temperature observations either from the GC-Net stations (Vandecrux et al.in review), at Dye-2 in 2016 (Heilig et al., 2018), at KAN_U (Charalampidis et al., 2015) and at the FA station (Koenig et al., 2014); ii) A collection of firn density profiles (Table S2); iii) The observation of percolation depth and liquid water content at Dye-2 over the summer 2016 (Heilig et al., 2018).

235 For firn density, we first compare the simulated density profiles to the firn core data. We also calculate for each time step the average firn density over the 0-1 m, 1-10 m and 10-20 m depth ranges and discuss the standard deviation of these values among models and their bias compared to punctual observations from firn cores. Hourly measurements of firn temperatures are compared to the interpolated temperature from the closest model layers. The Root Mean Squared Error (RMSE), mean bias and coefficient of determination (R^2) are then discussed to quantify the performance of the models in terms of firn

240 temperature.

4. Results

4.1. Firn density

The compared models do not always produce similar top 20 m firn density profiles (Figure 2). The site where density evolution is the most similar is at Summit and the differences between models is more visible at Dye-2 and KAN_U. At FA only one

245 melt season is investigated which is not enough for models' outputs to significantly diverge. At Dye-2, CFM-Cr, CFM-KM and UppsalaUniDeepPerc build up higher density firn from the surface to 10 m depth. In contrast, DTU, GEUS, IMAUFDM and UppsalaUniBucket simulate thinner high-density layers that are generated each summer at the surface and buried in the following months and years. Extremes (high or low) in density layers are harder to identify in DMIHH and MeyerHewitt. At

KAN_U, the simulated evolution of a pre-existing ice slab can be investigated in each model. The evolution of the density
250 profile at KAN_U depends on whether the model allows percolation past the ice slab (Figure 2). DMIHH and GEUS models
do not allow such percolation, and refreezing-related densification only occurs atop the ice slab. CFM-Cr, CFM-KM,
IMAUFDM, UppsalaUniBucket and UppsalaUniDeepPerc models percolate meltwater past the ice slab to 10-15 m. As a
result, the available pore space within the ice slab is used for refreezing (Figure 2). Nevertheless, the sealing of the ice slab in
these models does not prevent the meltwater from percolating through, and meltwater refreezing continues to occur at depth
255 and to densify the firn there.
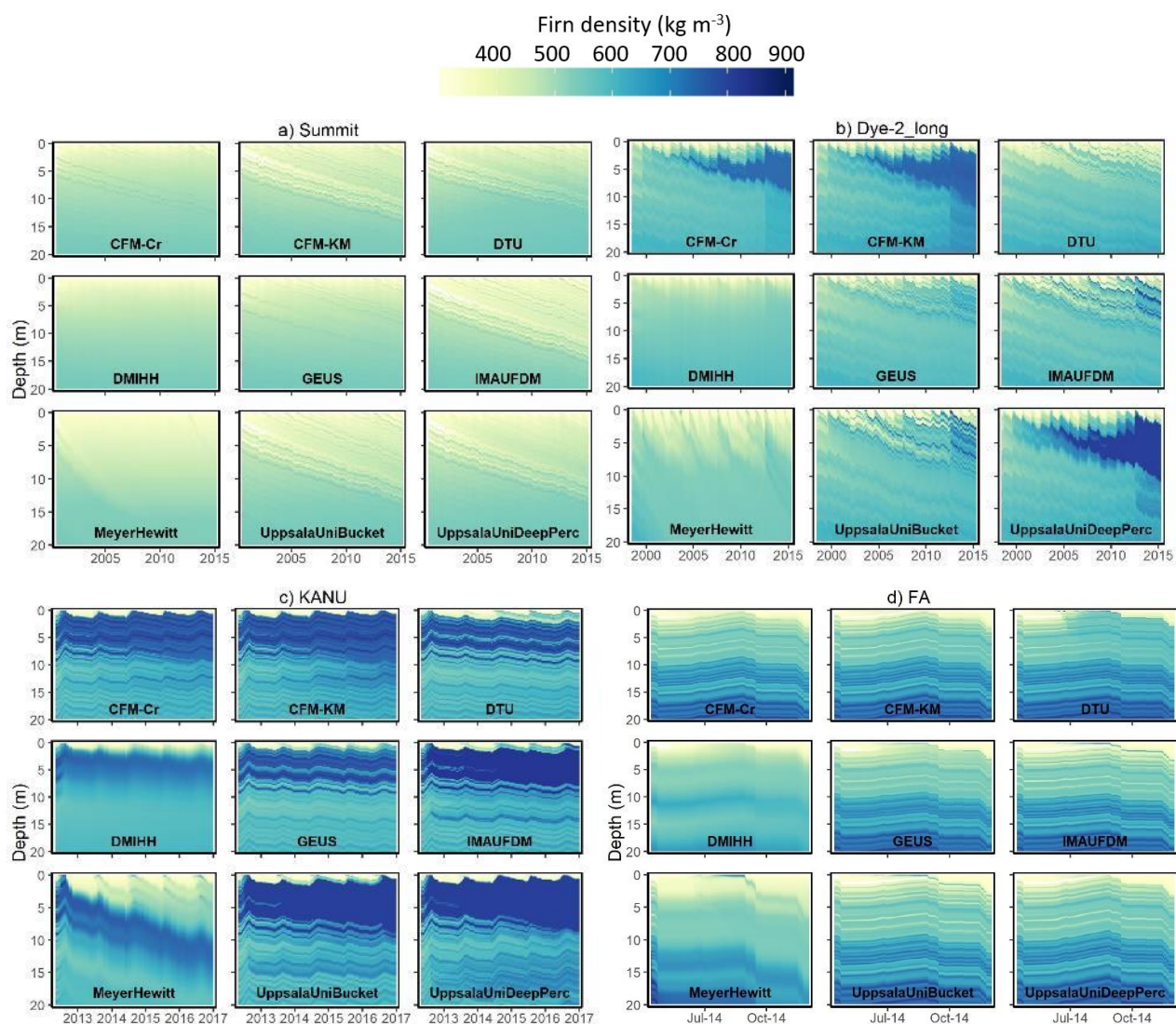
Figure 2: Simulated firn density at the four study sites.

260 At all sites, the models start with similar average densities due to the common initialisation (Figure 3). In the course of the
simulation, the standard deviation of simulated firn density values increases. At Summit, the models agree relatively well on

12

the average density independently of the depth range with a maximal standard deviation among models of 15 kg m^{-3} for the top 1 m average density, 27 kg m^{-3} for the 1-10 m range and 23 kg m^{-3} during the 15 year long simulation period. However, in the areas where more melt occurs, the differences between the simulated firn density are larger. At Dye-2, the maximum

265   standard deviation in top 1 m, 1-10 m and 10-20 m average firn densities are 161, 141 and 29 kg m^{-3} respectively. At KAN_U, the standard deviation in average firn density among models can be as high as 181 kg m^{-3} for the top 1 m, 110 kg m^{-3} for the 1-10 m depth range and 35 kg m^{-3} between 10 and 20 m depth. The models spread is highest close to the surface and diminish further at depth.

270
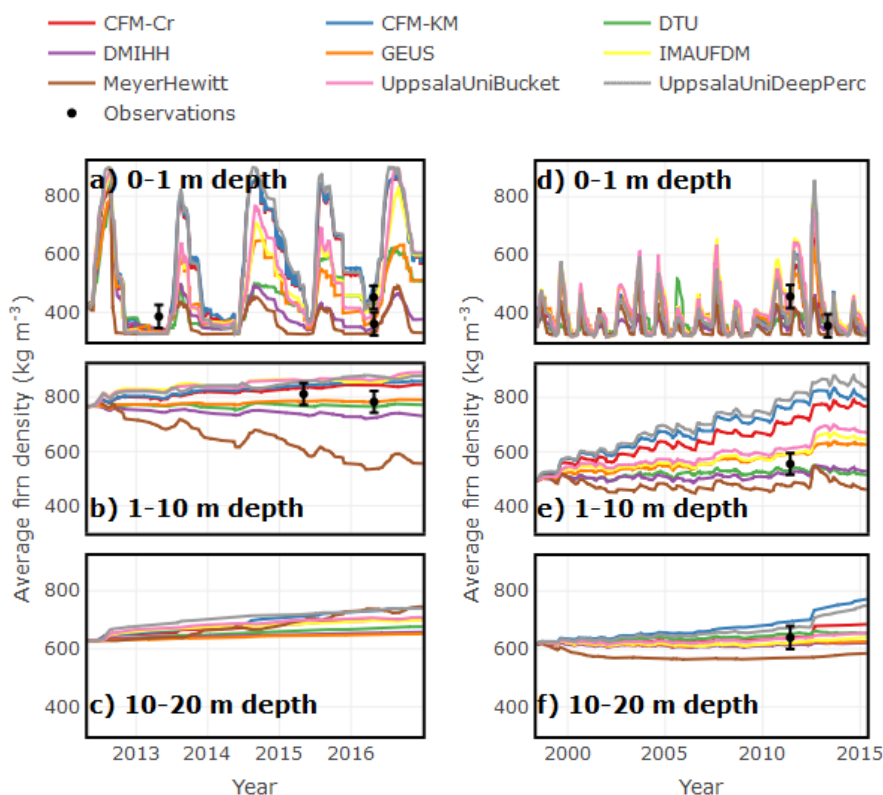
Figure 3: Modelled (coloured lines) and observed (black dots with 40 kg m-3 uncertainty bars) average firn density for the top 1 m (a,d), for the 1-10 m depth range (b,e) and 10-20 depth range (c,f) at KAN_U (a,b,c) and Dye-2 (d,e,f).

275   Comparison with firn cores from Summit in 2015, KAN_U in 2013 and 2016 and at Dye-2 in 2011 allow to identify the models that reach closest agreement with observations on specific dates. At Summit, all models reproduce the firn density within observation uncertainties (Figure 3). At KAN_U, the near-surface ice layer is prescribed at the initialization for all models in spring 2012. Most models still have this feature in 2016. Only MeyerHewitt and DMIHH model gradually smooth the initial density profile. Yet, they still simulate a firn layer of higher density at 5 m depth for DMIHH and around 12 m depth for MeyerHewitt. A low-density bias is also present in these two models close to the surface, both in 2013 and 2016.

280

13
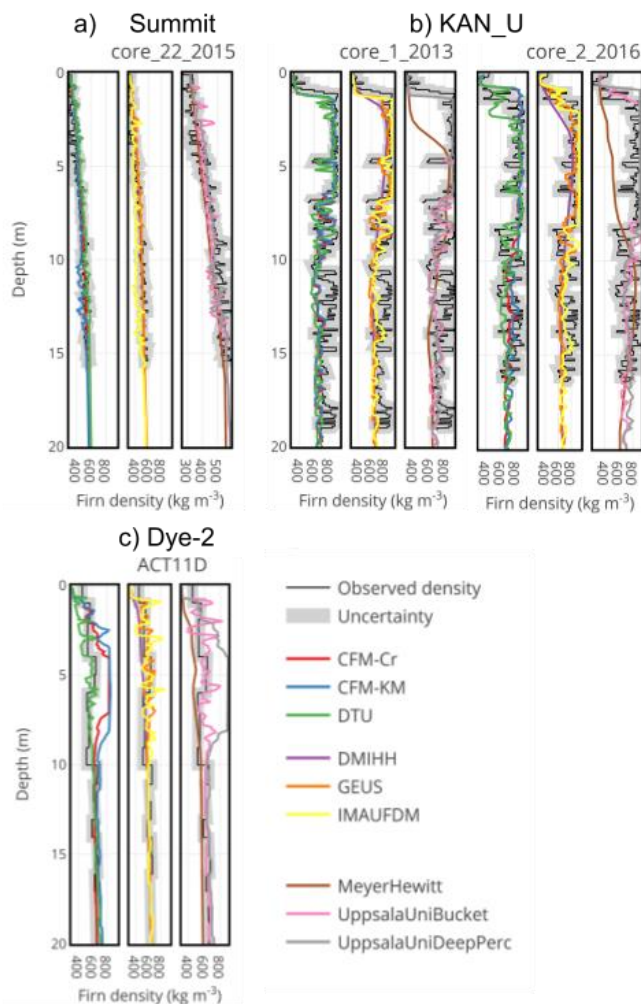
Figure 4: Observed and simulated density at Summit (a), KAN_U (b) and Dye-2 (c)

4.2. Firn temperature

Simulated firn temperature is most consistent among the 9 models at Summit, site with lowest melt. Given the same surface

285 forcing in terms of skin temperature, snowfall and sublimation and in the absence of meltwater infiltration, Summit provides

the opportunity of validating the capacity of the models to simulate heat conduction and advection through the firn. At Summit,

there are some visible differences between the models (Figure 5). MeyerHewitt is the model that propagates annual

temperature fluctuations the deepest. UppsalaUniDeepPerc allows the small amount of surface meltwater to percolate to depth

where it refreezes and releases latent heat. The DMIHH, GEUS, IMAU-FDM, UppsalaUniBucket are very similar at Summit.

290 The CFM models propagate heat slightly deeper than the previous models, but not as much as UppsalaUniDeepPerc.
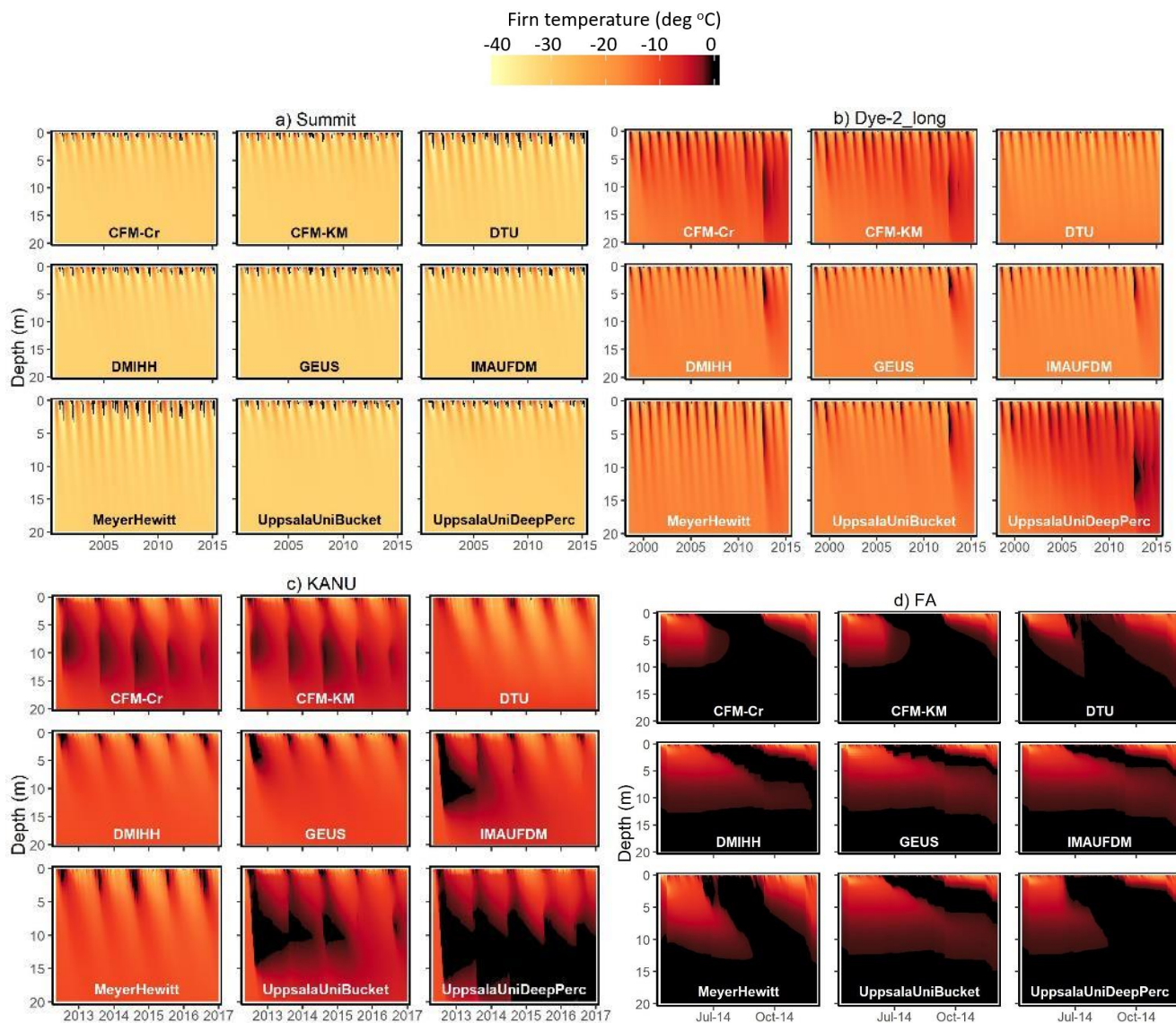
Figure 5: Simulated firn temperature at the four study sites.

295
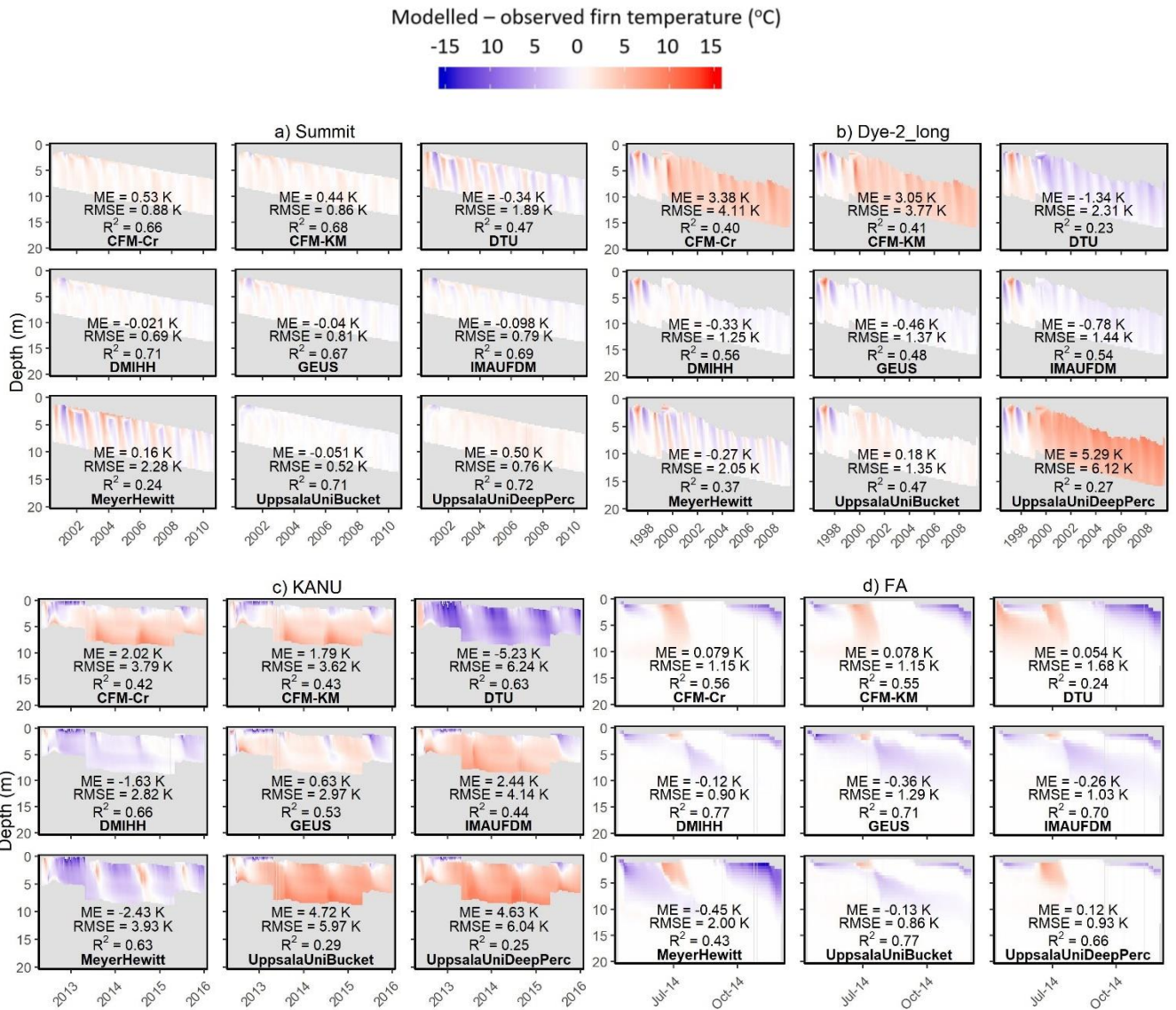
Figure 6: Deviation of simulated firn temperature from observations at the four study sites.

At Dye-2, the simulated firn temperatures are more model-dependent and their spread can be evaluated both on the long term with the 1998-2015 simulation as well as over the 2016 melting season with greater accuracy in the surface forcing (Figure 5). The spread in temperature can mainly be explained by the various meltwater routing schemes and will be discussed further in the next section.

The ability of the firn models to realistically simulate firn temperature is evaluated using the R^2, RMSE and ME statistics (Figure 6). Most models show a warm bias at Summit. At Dye-2, CFM-Cr, CFM-KM and UppsalaUniDeepPerc have a warm

16

310   bias while the other models can over- or under-estimate firn temperature depending on the season. At KAN_U, the DTU, DMIHH and MeyerHewitt have a cold bias, the GEUS bias show the lowest bias while all other models overestimate firn temperature. The case of FA is discussed in Section 5.3.

4.3. Meltwater percolation
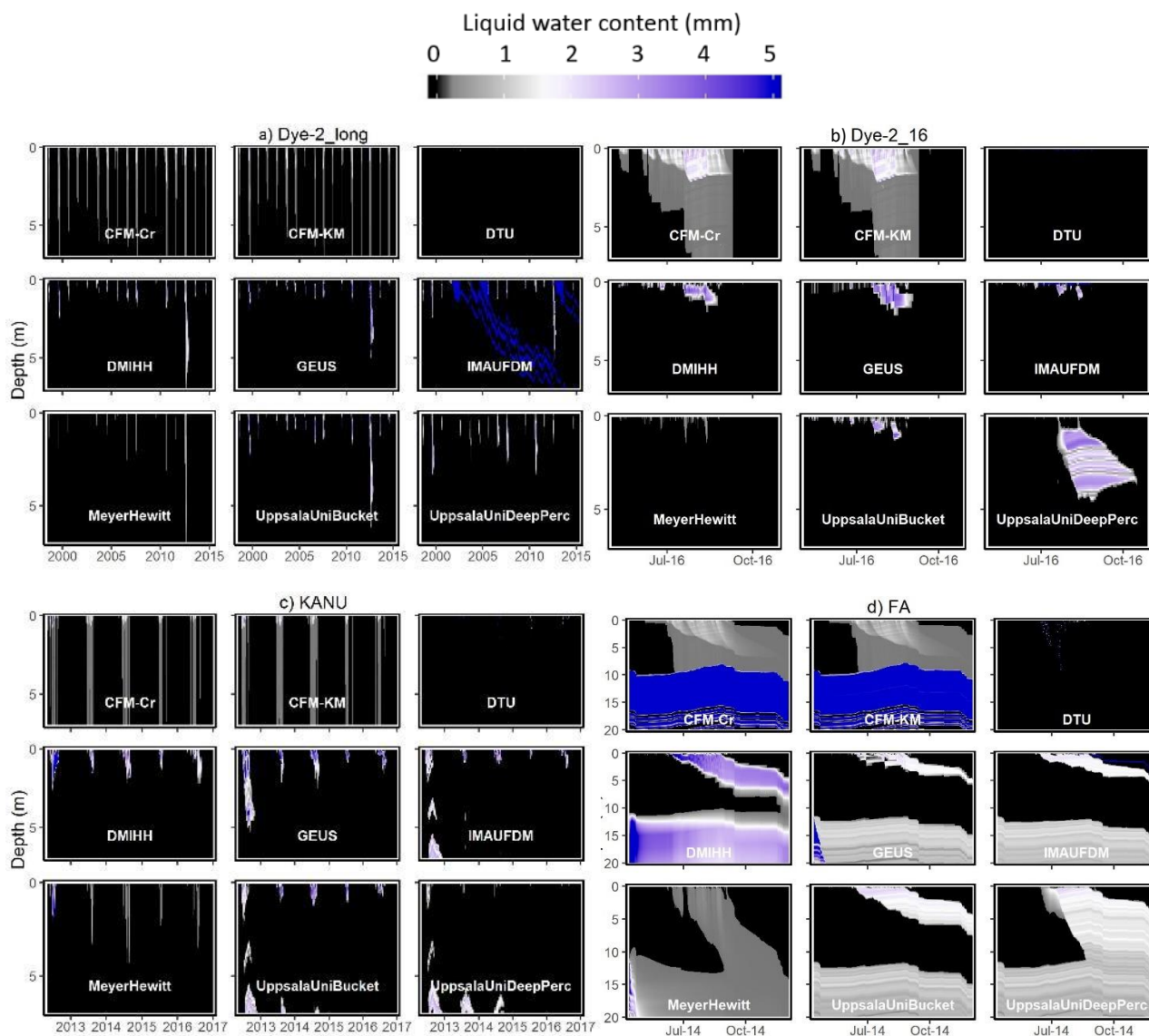
315

Figure 7: Simulated liquid water content at Dye-2 (a,b), KAN_U (c) and FA (d).

The high-quality forcing and boundary conditions available at Dye-2 over the 2016 melt season provides the best test situation

320   for the percolation schemes. The site has sufficient surface melt and the firn, although interspersed with ice layers, does not

prevent downward percolation. Simulated meltwater percolation depth varies greatly among the models (Figure 7). In the

DTU model, meltwater is only allowed in the top layer. This is due to the restriction of water not being able to penetrate ice

layers in the firn. UppsalaUniDeepPerc presents the deepest percolation. IMAUFDM and UppsalaUniBucket give similar

results and percolate water down to 2-3 m. The percolation pattern in CFM-Cr and CFM-KM is markedly different than all

325   other models with percolation down to 10 m. DMIHH and GEUS simulate similar maximum percolation depth with slightly

deeper percolation for GEUS model. The simulated firn density and temperature evolution for the 2016 melt season at Dye-2

are presented in Figure S4.
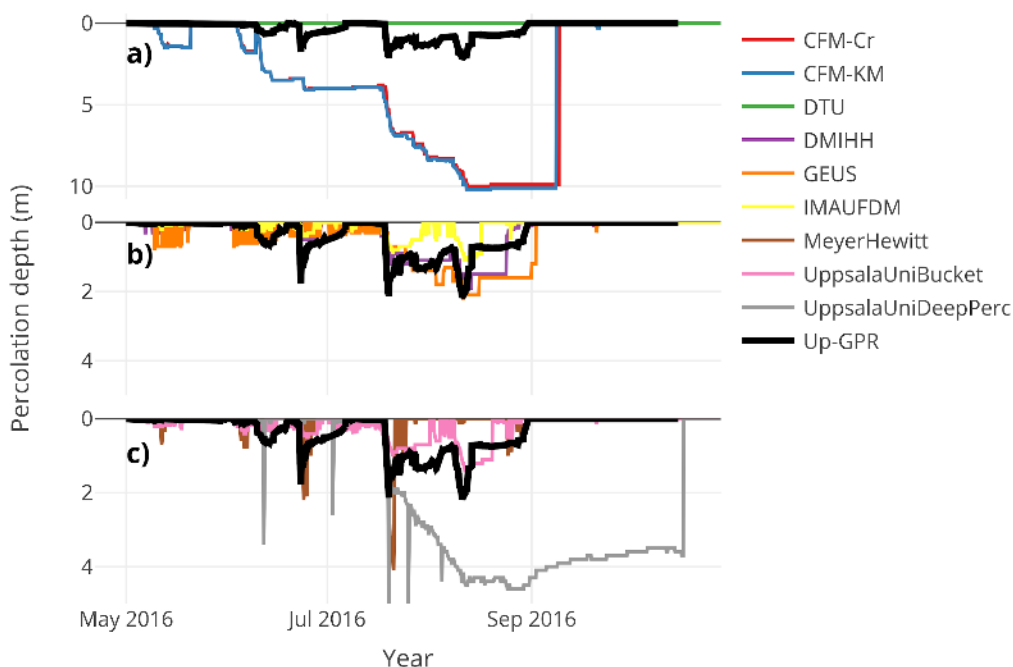
Figure 8: Comparison of the simulated (coloured lines) and observed (black line) meltwater percolation depth at Dye-2 over the
330   **2016 melting season.**

The observations from upward-looking ground penetrating radar (up-GPR) (Heilig et al., 2018) enable validating the

meltwater dynamics at Dye-2, a site representative of the percolation area of the Greenland ice sheet. Observations from up-

GPR show that the meltwater front did not reach below 2 m depth during the 2016 melt season. The melt was concentrated

around three periods of increasing intensity between May and June and a period when meltwater was continuously present in

335   the firn between 20 July and 25 September. We also note that the total melt for 2016 calculated from the up-GPR observation

is consistent with the melt amount derived from the weather station data and used to force all firn models, increasing our

confidence that firn models are here evaluated with forcing as close as possible to the in-situ weather. The CFM-CR and

CFM-KM models substantially overestimate percolation (Figure 8a, red and blue lines). The very large simulated percolation

depth (~10 m) can be attributed to the dual flow scheme, which exaggerates the effects of preferential flow. The other models

340   give a more percolation depth closer to observations.

5.   Discussion

5.1.   Impact of the model design on simulated density, temperature and water content

The variability in firn density, temperature and water content and the deviation between simulations and observations (Section 4) can be explained by the various ways physical processes are accounted for in the models. In this section we detail what can

345   be learned from the comparison and define potential improvement for future firn models.

5.1.1. Equivalence of the firn densification schemes at a dry snow site

At Summit, representative of dry snow conditions, this validation effort suggests that with appropriate forcing, the various densification laws perform similarly and within observational uncertainty. Our finding is not surprising as most of the densification schemes are calibrated against firn density profiles from dry snow areas. The good performance of firn models

350   in the dry snow area has been established from previous comparisons (Steger et al., 2017; Lundin et al., 2017; Alexander et al., 2019).

5.1.2. Bucket schemes, irreducible water content and ice slabs

IMAUFDM and UppsalaUniBucket have in common their bucket scheme and the use of irreducible water content by Coléou and Lesaffre (1998). They consequently present similar percolation depth at KAN_U and Dye-2 (Figure 7). IMAUFDM and

355   UppsalaUniBucket slightly underestimate percolation depth at Dye-2 in 2016 (Figure 8). This might be corrected by using a slightly lower irreducible water content. Indeed, the commonly used water content parametrization from Coléou and Lesaffre (1998) could be complemented by observations in natural firn or adapted to the specific needs of bucket scheme models. On the one hand, meltwater routing in bucket scheme models compare favourably to observations and to the DMIHH and GEUS models which include more advanced meltwater routing schemes (Figure 8). Yet again, the two bucket scheme models both

360   overestimate percolation at KAN_U in presence of an ice slab, evident from a warm bias there (Figure 6). Indeed, it was known that they can overestimate percolation depth and more advanced routing schemes show slightly better performance in simulating meltwater runoff from alpine snowpack (Wever et al. 2014). We therefore conclude that bucket schemes perform relatively well but accuracy in percolation depth could benefit from an improved representation of flow-impeding ice layers and from a slightly lower irreducible water content.

365

5.1.3. Numerical diffusion

In Lagrangian models, layers follow the firn as layers get buried under accumulating snow. In Eulerian models the firn is being transferred through fixed layers. Eulerian models such as DMIHH and MeyerHewitt, smooth the firn density profile and dissipate contrast in firn density (Figure 2). This appears to be independent of the model resolution since MeyerHewitt

370   has 18 times more layers than DMIHH. At KAN_U, these two models gradually lose the contrast between the layers that compose the ice slab and the firn below (Figure 2). Therefore, Eularian models tend to represent ice slabs in terms of a depth range with increased density, rather than marked layers of ice.

5.1.4. Deep percolation in low melt areas

At Summit, minimal amounts of meltwater are produced at the surface. Yet, the models that explicitly include deep percolation

375   (CFM-Cr, CFM-KM and UppsalaDeepPerc) present a warm bias (Figure 6). We interpret this as the signature of refreezing events at depth in the models. The deep percolation schemes seem less adapted for areas with minor melt until the conditions in which deep percolation occurs will be better constrained.

5.1.5. Spread in simulated firn temperature at Summit

In the dry snow zone where melt rarely occurs, temperature profiles are more strongly governed by the thermal conductivity

380   parameterization. At Summit, models produce slightly different firn temperature and DTU and MeyerHewitt models even show seasonal deviations compared to observations (Figure 6a). We see in this model spread the lack of agreement between various parameterizations of thermal conductivity. Errors due to inappropriate thermal conductivity propagate to firn temperature, densification rates and meltwater refreezing potential. Further work will therefore need to give better constrains to the firn thermal conductivity as.

385   ### 5.1.6. Ice slab creation at Dye-2 in deep percolation models

At Dye-2, more variations occur among the simulated density profiles (Figure 2). For instance, CFM-Cr, CFM-KM and UppsalaUniDeepPerc grow a several-meter-thick ice layer near the surface. The differing model behaviour can be explained by the simulation of water percolation bypassing ice layers and thus refreezing in cold underlying firn. The models that explicitly account for deep percolation (CFM-Cr, CFM-KM and UppsalaUniDeepPerc) all overestimate the near-surface firn

390   density at Dye-2.

5.1.7. Performance of the deep percolation schemes

The lack of preferential flow routine has recently been described as a caveat for firn models (e.g. van As et al., 2016). Yet, little is known about how often this phenomenon occurs in the firn, how deep meltwater is transported, nor which parameter or process triggers preferential flow. Here, the models that include deep percolation explicitly overestimate percolation depth and firn temperature at Summit and grow an ice slab at Dye-2. It therefore appears that a better understanding of deep percolation is needed before its inclusion in firn model becomes beneficial.

5.1.8. Insufficient heat at depth in the shallow percolation models

Models that keep meltwater close to the surface (DTU, DMIHH, GEUS, IMAUFDM, UppsalaUniBucket) also present a noticeable cold bias at most sites (Figure 6). The cold bias could be attributed to insufficient meltwater percolation. However, the validation at Dye-2 in 2016 indicates a reasonable percolation depth for all these models except DTU. Additionally, this cold bias is still present at Summit where little meltwater is available for percolation. We interpret these findings as an indication that heat transfer through the firn is still not accurately handled in most firn models. Especially, the heterogeneous nature of the firn, the presence of vertical ice features in the firn, the variability in surface snow density/thermal conductivity as well as firn ventilation are processes not currently included in the models and should be subject of future research.

5.1.9. Ice slab and impermeability threshold

At KAN_U, the DMIHH model gives the firn temperature with lowest RMSE and highest R^2 when compared to observations (Figure 6). The performance of DMIHH at KAN_U can be explained by the absence, in the simulation, of meltwater infiltration below the ice slab (Figure 7) which agrees with recent field evidences of the ice slabs' impermeability (MacFerrin et al., 2019). In DMIHH, the blocking of percolation originates from a simple permeability criterion: if a layer's density is higher than 810 kg m^{-3}, then the layer is impermeable, and any incoming meltwater is sent to runoff. The choice of this value was based on work in Antarctica which found that firn permeability reaches zero over a range of densities centred on 810 kg m^{-3} (Gregory et al., 2014). Unfortunately, no similar study is available in Greenland or in ice-saturated firn. The DTU model uses a similar threshold density to characterize a layer's impermeability but found that 917 kg m^{-3} gave the best match observed firn density profiles (Simonsen et al., 2013). On the contrary, the IMAU-FDM assumes that, at the horizontal resolution it usually operates (1-25 km^2), ice layers can be assumed discontinuous and are therefore never impermeable. Although we compare the models at KAN_U, few observations are available to evaluate these three approaches over a larger region or under different firn conditions. More work is therefore needed to quantify the permeability of ice-dominated firn in relation to the firn density, the ice layer thickness and the various spatial and temporal scale at which the firn models are used.

5.1.10. Fresh snow density

In this study, we used a constant density at which new snow is added to the top of the model columns. However, modelling studies revealed that the fresh snow density parameter significantly impacts the simulated firn densities (Steger et al., 2017; van Kampenhout et al., 2017; Alexander et al., 2019). Historically, parameterizations have been constructed on observations of the top 1 m snow density (Reeh et al., 2005; Kuipers Munneke et al., 2015). Other values such as 344-350 kg m3 were used in Svalbard by Van Pelt et al. (2014; 2019), a density of 400 kg m^{-3} has been used by Charalampidis et al. (2015) on the Greenland ice sheet and Verjans et al. (2019) used values between 240 and 365 kg m^3 based on site-specific observations. Fausto et al. (2018) concluded from a large Greenland dataset that no robust parametrization could be found based on mean annual air temperature, mean annual accumulation, elevation, latitude or longitude. For this reason, we here use a site-invariant fresh snow density of 315 kg m^{-3} (Fausto et al., 2018). The use of this fresh snow value was found to improve the result of a firn model in Greenland (Steger et al., 2017). A constant value is nevertheless far from the observed variability and leads to an overly simplistic boundary condition for densification schemes. Additionally, inaccurate fresh snow density can have drastic impact on the heat transfer through the very top of the snowpack. Hence, it is necessary to develop our understanding of fresh snow density in firn models and how this boundary condition may interact with the densification and heat transfer scheme.

5.2. Uncertainty in model-derived firn characteristics and mass balance

5.2.1. Uncertainty applying to simulated firn characteristics

Given the complexity of the firn models, it is hard to propagate uncertainty and account for model assumptions and parameterisations. As a consequence, model results have commonly been given without uncertainty range which prevents assessing the strength of model-based inferences. We see from Figure 2 to 7 that the spread between models increases as we move from the dry snow area to the percolation area, peaking in areas with high-melt features such as ice slabs and firn aquifers. We suggest that the model spread presented here can provide a baseline for uncertainty whenever a single model is used. At Summit, representative of the dry snow area, the standard deviation across models of average density in the 1-10 m depth range is 27 kg m^{-3}. Hence, an uncertainty envelope of ±60kg m^{-3} can be used to describe the modelling uncertainty. At, Dye-2, representative of the percolation area, models have a standard deviation of 141 kg m^{-3} at the end of the 15 year-long simulation. This indicates a substantial level of uncertainty (±280 kg m^{-3}) that applies to simulated firn densities in the percolation area. In the same way as for density, the models' spread in simulated firn temperature can be investigated by calculating the standard deviation in average firn temperature for the top 1 m, 1-10 m and 10-20 m depth range (Figure S5). At Summit the model spread is largest close to the surface with a standard deviation of 7ºC. This implies an uncertainty envelope of ±14ºC. This model uncertainty envelope increases with melt to ±15ºC at Dye-2 and ±18ºC at KAN_U and decreases with depth with an uncertainty envelope of ±8ºC on the 10-20 m average firn temperature. These uncertainties

applying to simulated firn density and temperature represent model-based estimates and would apply in the absence of observations to evaluate model performance directly.

5.2.2. Uncertainty in modelled mass balance

All the models agree on the total refreezing of meltwater at Summit. At other sites, the difference in simulated firn density,
455   temperature and the liquid water distribution cause the models to allow different amounts of meltwater to refreeze and runoff and therefore affect the surface mass balance.

At KAN_U, for instance, the impact of the ice slab on the surface mass balance is critical. The differing simulated percolation patterns lead to varying total amounts of meltwater either refrozen or runoff (Figure 7 and 9). The bucket schemes in
460   IMAUFDM and UppsalaUniBucket percolate meltwater through the firn and all the meltwater refreezes below the ice slab in these models. The deep percolation scheme in UppsalaDeepPerc leads to the same result. In the CFM models, the Richards equation in the matrix flow domain prescribes relatively slow meltwater percolation through the ice layer and the preferential flow domain is unable to accommodate all the incoming water. As a result, part of the meltwater is sent to lateral runoff. In all the other models, the presence of ice layers triggers meltwater ponding and runoff. In 2012, the DTU model presents the
465   highest runoff, followed by the DMIHH model. In the following years, only DTU, CFM-Cr, CFM-KM and DMIHH models still calculate minor runoff. Machguth et al. (2016) calculated from firn cores that a $75 \pm 15\%$ of the surface meltwater went to runoff at KAN_U in 2012. Although the observations are subject to considerable uncertainty, they indicate that most of the models underestimate the runoff at KAN_U in 2012.

470   At Dye-2, all models agree that runoff is minimal compared to refreezing. Yet most models, except the ones using bucket schemes (IMAUFDM and UppsalaUniBucket), indicate that runoff occurs regularly. Runoff peaked in all models in 2012, when above average melt was available at the surface. If melt continues to increase and the near-surface firn permeability further decrease, Dye-2 has the potential to turn into an ice slab site as hypothesized by Vandecrux et al. (2018, 2019).
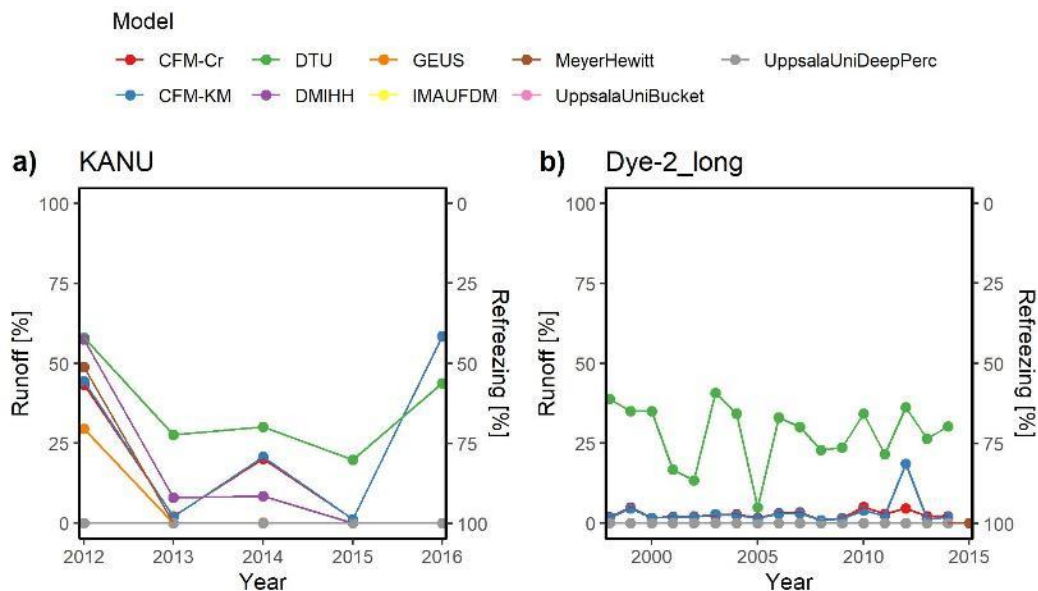
Figure 9. Yearly totals for meltwater runoff and refreezing at KAN_U (a) and Dye-2 (b).

5.3. Firn aquifer

5.3.1. Subsurface runoff at a firn aquifer site

The presence of water in excess of irreducible water content is not allowed in some of the models: IMAUFDM, Uppsala. This implies that, at the initiation of these models, all the excess water within the aquifer is sent to runoff instantaneously. The DMIHH model runs off excess water according to the parametrization by Zuo and Oerlemans (1996). This leads to the gradual decrease of water content within the aquifer. The GEUS model incorporates a Darcy-like parametrization of the subsurface runoff and calculates much faster drainage of the aquifer.

5.3.2. Representation of aquifers in firn models

Aquifers are currently poorly represented in models, which poses the question of the suitability of the models to simulate aquifers in Greenland. Forster et al. (2015) used the output from RACMO to map aquifer over the entire ice sheet. However, the RACMO RCM, using the IMAUFDM firn model, is incapable of modelling actual aquifer (defined as saturated firn). Instead, areas where the model showed residual subsurface water (within the irreducible water content) remaining in spring was used as an indicator of areas where firn aquifers might be present. Although this approach succeeds at mapping the current firn aquifer areas, the difference between what is tracked in the model and what actually happens at firn aquifer puts doubt on the current capacity of firn models to predict firn aquifer evolution in future climate. In reality, horizontal water flow at depth

plays a crucial role in the evolution of firn aquifers. However, current firn models are one-dimensional. As such, lateral water movement is governed by poorly constrained parameterizations, which are unlikely to accurately represent horizontal flow.

5.3.3. Recharge of the firn aquifer

495

500

Another challenging question for our understanding of these aquifer sites is: Where and when does the meltwater generated at the surface percolate down to the aquifer? Firn temperature observations (Figure S3) show that the top 20 m of firn remained at melting point during the 2014 melt season. This indicates that meltwater from the surface reached the aquifer. The firn models do not conclusively answer how and where deep percolation to the firn aquifer takes place. Given the same surface forcing and initial firn conditions, few of the models: CFM-Cr, CFM-KM, UppsalaUniBucket and UppsalaUniDeepPerc, route water past 10 m depth. These are the models that use either a dedicated deep percolation scheme or a bucket-type routing scheme within which the irreducible water content might be set to account for deep percolation.

6. Conclusions

505

Nine state-of-the-art firn models are forced with mass and energy fluxes calculated from weather station data at four sites representative of various climate zones of the Greenland ice sheet. From the comparison of their simulated firn temperature, density and water content and from the validation against various firn observations, we identify specific routines within the models that are responsible for the models' behaviours. We later quantify uncertainties that apply to the firn model outputs and identify key topics for future development of models and for the investigation of firn processes.

510

515

520

Model spread and deviation between simulated and observed firn density and temperature is largest at the sites that experience more melt. Using twice the models' standard deviation as an indicator of uncertainty envelop, we find that firn models can estimate firn density within ± 60 kg m^{-3} at a dry snow site and that uncertainty increases to ± 280 kg m^{-3} for certain depth ranges at percolation sites. Runoff-enhancing ice slabs were formed in certain models at the Dye-2 site where they were not observed. At the KAN_U site, where models were initialized with multi-meter ice layer according to observations, models did not agree on whether meltwater could percolate through. Eulerian models appear to smooth the firn density profile and dissipate contrast in firn density independently of the model resolution. Further testing of such models should investigate how this numerical diffusion affect the firn characteristics over longer runs and in particular how runoff-enhancing ice slabs are represented in these models. The good performance of all models at the nearly-melt-free Summit site indicates that for the top 20 m of firn, the densification laws perform similarly under dry snow conditions given identical forcing. Variability in simulated firn temperature at Summit indicates that heat transfer through the firn is still not handled consistently in firn models. The heterogeneous nature of the firn, the presence of vertical ice features in the firn, the variability in surface snow density/thermal conductivity as well as firn ventilation are processes not currently included in the models and should be subject of future research.

The Cryosphere
Discussions

Differences in simulated firn characteristics lead to different amounts of meltwater retained through refreezing or escaping the site through runoff. Models that percolate meltwater deeper (resp. shallower) calculate higher (resp. lower) retention through refreezing and therefore less (resp. more) lateral runoff. Models that include explicit deep percolation schemes did not compare better to observations of firn temperature and of meltwater percolation at an ice slab site. Yet they were able to simulate successfully meltwater percolation at ~10 m depth at a firn aquifer site. At that aquifer site, models that used the Darcy's law and bucket schemes did not percolate meltwater deep enough to recharge the aquifer but presented satisfactory results at a cold firn site. Only the models using Darcy's law compared favourably to observation at the ice slab site. These mixed results show that even the latest models need development to perform satisfactorily under multiple climate and with various firn structure. This can only be done with better laboratory and in situ observations of both horizontal and vertical flow of water in firn and by an understanding of how the spatial representativity of firn models.

Prescription of fresh snow density and snow grain size are yet to be investigated as they are expected to have an important impact on the model outputs. Future measurement campaigns and modelling efforts could help to understand how these quantities interact with the densification and heat transfer scheme.

7. Data availability

The forcing datasets as well as all the model outputs is available on https://www.promice.org/PromiceDataPortal/. The code for all the plots are available on https://github.com/BaptisteVandecrux/RetMIP. The source code for the CFM model is available at https://github.com/UWGlaciology/CommunityFirnModel; the GEUS model code can be found at https://github.com/BaptisteVandecrux/SEB_Firn_model. The RetMIP protocol is available at http://retain.geus.dk/index.php/retmip/.

8. Funding

References

550 Ahlstrøm, A. P., Gravesen, P., Andersen, S. B., van As, D., Citterio, M., Fausto, R. S., Nielsen, S., Jepsen, H. F., Kristensen, S. S., Christensen, E. L., Stenseng, L., Forsberg, R., Hanson, S. and Petersen, D.: A new programme for monitoring the mass loss of the Greenland ice sheet, Geol. Surv. Denmark Greenl. Bull., (15), 61–64 http://www.geus.dk/DK/publications/geol-survey-dk-gl-bull/15/Documents/nr15_p61-64.pdf , 2008.

Alexander, P. M., Tedesco, M., Koenig, L. and Fettweis, X.: Evaluating a Regional Climate Model Simulation of Greenland
555 Ice Sheet Snow and Firn Density for Improved Surface Mass Balance Estimates, Geophys. Res. Lett., 46(21), 12073–12082, https://doi.org/10.1029/2019GL084101, 2019.

Anderson, E. A.: A point energy and mass balance model of a snow cover. [online] Available from: http://www.csa.com/partners/viewrecord.php?requester=gs&collection=ENV&recid=7611864%5Cnhttp://www.agu.org/pubs/crossref/2009/2009JD011949.shtml, 1976.

560 Arthern, R. J., Vaughan, D. G., Rankin, A. M., Mulvaney, R. and Thomas, E. R.: In situ measurements of Antarctic snow compaction compared with predictions of models, J. Geophys. Res. Earth Surf., 115(3), 1–12, https://doi.org/10.1029/2009JF001306, 2010.

Benson, C.S.: Stratigraphic studies in the snow and firn of the Greenland ice sheet. SIPRE Res. Rep. 70, 76–83, 1962.

Box, J. E.: Greenland ice sheet mass balance reconstruction. Part II: Surface mass balance (1840-2010), J. Clim., 26(18),
565 6974–6989, https://doi.org/10.1175/JCLI-D-12-00518.1, 2013.

Box, J. E., Cressie, N., Bromwich, D. H., Jung, J. H., Van Den Broeke, M., Van Angelen, J. H., Forster, R. R., Miège, C., Mosley-Thompson, E., Vinther, B. and Mcconnell, J. R.: Greenland ice sheet mass balance reconstruction. Part I: Net snow accumulation (1600-2009), J. Clim., 26(11), 3919–3934, https://doi.org/10.1175/JCLI-D-12-00373.1, 2013.

Braithwaite, R. J., Laternser, M. and Pfeffer, W. T.: Variations of near-surface firn density in the lower accumulation area of
570 the Greenland ice sheet, Pakitsoq, West Greenland, J. Glaciol., 40(136), 477–485, https://doi.org/10.1017/S002214300001234X, 1994.

Calonne, N., Flin, F., Morin, S., Lesaffre, B., Du Roscoat, S. R. and Geindreau, C.: Numerical and experimental investigations of the effective thermal conductivity of snow, Geophys. Res. Lett., 38(23), 1–6, https://doi.org/10.1029/2011GL049234, 2011.

Calonne, N., Geindreau, C., Flin, F., Morin, S., Lesaffre, B., Roscoat, S. R. and Charrier, P. : 3-D image-based numerical
575 computations of snow permeability: Links to specific surface area, density, and microstructural anisotropy. Cryosphere, 6(5), 939–951, https://doi.org/ 10.5194/tc-6-939-2012, 2012.

Charalampidis, C., Van As, D., Box, J. E., Van Den Broeke, M. R., Colgan, W. T., Doyle, S. H., Hubbard, A. L., MacFerrin, M., Machguth, H. and P. Smeets, C. J. P.: Changing surface-atmosphere energy exchange and refreezing capacity of the lower accumulation area, West Greenland, Cryosphere, 9(6), 2163–2181, https://doi.org/10.5194/tc-9-2163-2015, 2015.

580 Colbeck, S. C.: A theory for water flow through a layered snowpack, Water Resour. Res., 11(2), 261–266, https://doi.org/10.1029/WR011i002p00261, 1975.

Coléou, C. and Lesaffre, B.: Irreducible water saturation in snow: experimental results in a cold laboratory, Ann. Glaciol., 26(2), 64–68, https://doi.org/10.3189/1998aog26-1-64-68, 1998.

Fausto, R. S., Ahlstrøm, A. P., Van As, D., Johnsen, S. J., Langen, P. L. and Steffen, K.: Improving surface boundary

585   conditions with focus on coupling snow densification and meltwater retention in large-scale ice-sheet models of Greenland, J. Glaciol., 55(193), 869–878, https://doi.org/10.3189/002214309790152537, 2009.

Goujon, C., Barnola, J. M. and Ritz, C.: Modelling the densification of polar firn including heat diffusion: Application to close-off characteristics and gas isotopic fractionation for Antarctica and Greenland sites, J. Geophys. Res. D Atmos., 108(24), n/a-n/a, https://doi.org/10.1029/2002jd003319, 2003.

590   Gregory, S. A., Albert, M. R., and Baker, I.: Impact of physical properties and accumulation rate on pore close-off in layered firn. Cryosphere 8, 91–105. https://doi.org/10.5194/tc-8-91-2014. 2014.

Heilig, A., Eisen, O., MacFerrin, M., Tedesco, M., and Fettweis, X.: Seasonal monitoring of melt and accumulation within the deep percolation zone of the Greenland Ice Sheet and comparison with simulations of regional climate modeling, The Cryosphere, 12, 1851–1866, https://doi.org/10.5194/tc-12-1851-2018, 2018.

595   Herron, M. M. and Langway, C. C.: Firn Densification: An Empirical Model, J. Glaciol., 25(93), 373–385, https://doi.org/10.3189/s0022143000015239, 1980.

Hirashima, H., Yamaguchi, S., Sato, A. and Lehning, M.: Numerical modeling of liquid water movement through layered snow based on new measurements of the water retention curve, Cold Reg. Sci. Technol., 64(2), 94–103, https://doi.org/10.1016/j.coldregions.2010.09.003, 2010.

600   Howat, I. M., Negrete, A. and Smith, B. E.: The Greenland Ice Mapping Project (GIMP) land classification and surface elevation data sets, Cryosphere, 8(4), 1509–1518, https://doi.org/10.5194/tc-8-1509-2014, 2014.

Kameda, T., Narita, H., Shoji, H., Nishio, F., Fujii, Y. and Watanabe, O.: Melt features in ice cores from Site J, southern Greenland: some implications for summer climate since AD 1550, Ann. Glaciol., 21, 51–58, https://doi.org/10.3189/s0260305500015597, 1995.

605   Katsushima, T., Kumakura, T. and Takeuchi, Y.: A multiple snow layer model including a parameterization of vertical water channel process in snowpack, Cold Reg. Sci. Technol., 59(2–3), 143–151, https://doi.org/10.1016/j.coldregions.2009.09.002, 2009.

Koenig, L. S., Miège, C., Forster, R. R. and Brucker, L.: Initial in situ measurements of perennial meltwater storage in the Greenland firn aquifer, Geophys. Res. Lett., 41(1), 81–85, https://doi.org/10.1002/2013GL058083, 2014.

610   Kuipers Munneke, P., Ligtenberg, S. R. M., Noël, B. P. Y., Howat, I. M., Box, J. E., Mosley-Thompson, E., McConnell, J. R., Steffen, K., Harper, J. T., Das, S. B. and Van Den Broeke, M. R.: Elevation change of the Greenland Ice Sheet due to surface mass balance and firn processes, 1960-2014, Cryosphere, 9(6), 2009–2025, https://doi.org/10.5194/tc-9-2009-2015, 2015.

Lefebre, F., Gallée, H., van Ypersele, J.-P. and Greuell, W.: Modeling of snow and ice melt at ETH Camp (West Greenland):

615   A study of surface albedo, J. Geophys. Res., 108(D8), 4231, https://doi.org/10.1029/2001JD001160, 2003

Ligtenberg, S. R. M., Helsen, M. M. and Van Den Broeke, M. R.: An improved semi-empirical model for the densification of Antarctic firn, Cryosphere, 5(4), 809–819, https://doi.org/10.5194/tc-5-809-2011, 2011.

Ligtenberg, S. R. M., Munneke, P. K., Noël, B. P. Y. and Van Den Broeke, M. R.: Brief communication: Improved simulation of the present-day Greenland firn layer (1960-2016), Cryosphere, 12(5), 1643–1649, https://doi.org/10.5194/tc-12-1643-2018, 2018.

Lundin, J. M. D., Stevens, C. M., Arthern, R., Buizert, C., Orsi, A., Ligtenberg, S. R. M., Simonsen, S. B., Cummings, E., Essery, R., Leahy, W., Harris, P., Helsen, M. M. and Waddington, E. D.: Firn Model Intercomparison Experiment (FirnMICE), J. Glaciol., 63(239), 401–422, https://doi.org/10.1017/jog.2016.114, 2017.

MacFerrin, M., Machguth, H., As, D. van, Charalampidis, C., Stevens, C. M., Heilig, A., Vandecrux, B., Langen, P. L., Mottram, R., Fettweis, X., Van Den Broeke, M. R., Pfeffer, W. T., Moussavi, M. S. and Abdalati, W.: Rapid expansion of Greenland's low-permeability ice slabs, Nature, 573(7774), 403–407, https://doi.org/10.1038/s41586-019-1550-3, 2019.

Machguth, H., Macferrin, M., Van As, D., Box, J. E., Charalampidis, C., Colgan, W., Fausto, R. S., Meijer, H. A. J., Mosley-Thompson, E. and Van De Wal, R. S. W.: Greenland meltwater storage in firn limited by near-surface ice formation, Nat. Clim. Chang., 6(4), 390–393, https://doi.org/10.1038/nclimate2899, 2016.

Marchenko, S., Van Pelt, W. J. J., Claremar, B., Pohjola, V., Pettersson, R., Machguth, H. and Reijmer, C.: Parameterizing deep water percolation improves subsurface temperature simulations by a multilayer firn model, Front. Earth Sci., 5(March), https://doi.org/10.3389/feart.2017.00016, 2017.

Mayewski, P. and Whitlow S.: Snow Pit Data from Greenland Summit, 1989 to 1993, NSF Arctic Data Center, https://doi.org/10.5065/D6NP22KX, 2016b.

Meyer, C. R. and Hewitt, I. J.: A continuum model for meltwater flow through compacting snow, Cryosphere, 11(6), 2799–2813, https://doi.org/10.5194/tc-11-2799-2017, 2017.Miège, C., Forster, R. R., Brucker, L., Koenig, L. S., Solomon, D. K., Paden, J. D., Box, J. E., Burgess, E. W., Miller, J. Z., McNerney, L., Brautigam, N., Fausto, R. S. and Gogineni, S.: Spatial extent and temporal variability of Greenland firn aquifers detected by ground and airborne radars, J. Geophys. Res. Earth Surf., 121(12), 2381–2398, https://doi.org/10.1002/2016JF003869, 2016.

Miller, O., Solomon, D. K., Miège, C., Koenig, L., Forster, R., Schmerr, N., Ligtenberg, S. R. M. and Montgomery, L.: Direct Evidence of Meltwater Flow Within a Firn Aquifer in Southeast Greenland, Geophys. Res. Lett., 45(1), 207–215, https://doi.org/10.1002/2017GL075707, 2018.

Montgomery, L., Koenig, L. and Alexander, P.: The SUMup dataset: Compiled measurements of surface mass balance components over ice sheets and sea ice with analysis over Greenland, Earth Syst. Sci. Data, 10(4), 1959–1985, https://doi.org/10.5194/essd-10-1959-2018, 2018.

Mosley-Thompson, E., McConnell, J. R., Bales, R. C., Li, Z., Lin, P. N., Steffen, K., Thompson, L. G., Edwards, R. and Bathke, D.: Local to regional-scale variability of annual net accumulation on the Greenland ice sheet from PARCA cores, J. Geophys. Res. Atmos., 106(D24), 33839–33851, https://doi.org/10.1029/2001JD900067, 2001.

Noël, B., Van De Berg, W. J., Van Wessem, J. M., Van Meijgaard, E., Van As, Di., Lenaerts, J. T. M., Lhermitte, S., Munneke, P. K., Smeets, C. J. P. P., Van Ulft, L. H., Van De Wal, R. S. W. and Van Den Broeke, M. R.: Modelling the climate and

surface mass balance of polar ice sheets using RACMO2 - Part 1: Greenland (1958-2016), Cryosphere, 12(3), 811–831, https://doi.org/10.5194/tc-12-811-2018, 2018.

Pfeffer, W. T., Meier, M. F. and Illangasekare, T. H.: Retention of Greenland runoff by refreezing: implications for projected future sea level change, J. Geophys. Res., 96(C12), 22117, https://doi.org/10.1029/91jc02502, 1991.

655 Polashenski, C., Courville, Z., Benson, C., Wagner, A., Chen, J., Wong, G., Hawley, R. and Hall, D.: Observations of pronounced Greenland ice sheet firn warming and implications for runoff production, Geophys. Res. Lett., 41(12), 4238–4246, https://doi.org/10.1002/2014GL059806, 2014.

Reeh, N., Fisher, D. A., Koerner, R. M. and Clausen, H. B.: An empirical firn-densification model comprising ice lenses, Ann. Glaciol., 42, 101–106, https://doi.org/10.3189/172756405781812871, 2005.

660 Reijmer, C. H., Van Den Broeke, M. R., Fettweis, X., Ettema, J. and Stap, L. B.: Refreezing on the Greenland ice sheet: A comparison of parameterizations, Cryosphere, 6(4), 743–762, https://doi.org/10.5194/tc-6-743-2012, 2012.

Samimi, S. and Marshall, S. J.: Diurnal cycles of meltwater percolation, refreezing, and drainage in the supraglacial snowpack of Haig Glacier, Canadian Rocky Mountains, Front. Earth Sci., 5(February), 1–15, https://doi.org/10.3389/feart.2017.00006, 2017.

665 Schneider, T. and Jansson, P.: Internal accumulation in firn and its significance for the mass balance of Storglaciären, Sweden, J. Glaciol., 50(168), 25–34, https://doi.org/10.3189/172756504781830277, 2004.

Schwander, J., Sowers, T., Barnola, J.M., Blunier, T., Fuchs, A. and Malaizé, B.: Age scale of the air in the Summit ice: implication for glacial–interglacial temperature change. J. Geophys. Res., 102(D16), 19 483–19 493, 1997.

Simonsen, S. B., Stenseng, L., Adalgeirsdóttir, G., Fausto, R. S., Hvidberg, C. S. and Lucas-Picher, P.: Assessing a
670 multilayered dynamic firn-compaction model for Greenland with ASIRAS radar measurements, J. Glaciol., 59(215), 545–558, https://doi.org/10.3189/2013JoG12J158, 2013.

Spencer, M. K., Alley, R. B. and Creyts, T. T.: Preliminary firn-densification model with 38-site dataset, J. Glaciol., 47(159), 671–676, https://doi.org/10.3189/172756501781831765, 2001.

Steffen, C., Box, J. and Abdalati, W.: Greenland Climate Network: GC-Net., 1996.Steger, C. R., Reijmer, C. H. and Van Den
675 Broeke, M. R.: The modelled liquid water balance of the Greenland Ice Sheet, Cryosphere, 11(6), 2507–2526, https://doi.org/10.5194/tc-11-2507-2017, 2017.

Stevens, C. M., Verjans, V., Lundin, J. M. D., Kahle, E. C., Horlings, A. N., Horlings, B. I., and Waddington, E. D.: The Community Firn Model (CFM) v1.0, Geosci. Model Dev. Discuss., https://doi.org/10.5194/gmd-2019-361, in review, 2020.

Steger, C. R., Reijmer, C. H., van den Broeke, M. R., Wever, N., Forster, R. R., Koenig, L. S., Munneke, P. K., Lehning, M.,
680 Lhermitte, S., Ligtenberg, S. R. M., Miège, C. and Noël, B. P. Y.: Firn meltwater retention on the Greenland ice sheet: A model comparison, Front. Earth Sci., 5(January), https://doi.org/10.3389/feart.2017.00003, 2017.

Sturm, M., Holmgren, J., König, M. and Morris, K.: The thermal conductivity of seasonal snow, J. Glaciol., 43(143), 26–41, https://doi.org/10.1017/S0022143000002781, 1997.

Sørensen, L. S., Simonsen, S. B., Nielsen, K., Lucas-Picher, P., Spada, G., Adalgeirsdottir, G., Forsberg, R. and Hvidberg, C.

685   S.: Mass balance of the Greenland ice sheet (2003-2008) from ICESat data - The impact of interpolation, sampling and firn density, Cryosphere, 5(1), 173–186, https://doi.org/10.5194/tc-5-173-2011, 2011.

Team, T. I.: Mass balance of the Greenland Ice Sheet from 1992 to 2018, Nature, https://doi.org/10.1038/s41586-019-1855-2, 2019.

Van Angelen, J. H., Lenaerts, J. T. M., Van Den Broeke, M. R., Fettweis, X. and Van Meijgaard, E.: Rapid loss of firn pore

690   space accelerates 21st century Greenland mass loss, Geophys. Res. Lett., 40(10), 2109–2113, https://doi.org/10.1002/grl.50490, 2013.

Van As, D., Mikkelsen, A. B., Nielsen, M. H., Box, J. E., Liljedahl, L. C., Lindbäck, K., Pitcher, L. and Hasholt, B.: Hypsometric amplification and routing moderation of Greenland ice sheet meltwater release, Cryosphere, 11(3), 1371–1386, https://doi.org/10.5194/tc-11-1371-2017, 2017.

695   Van As, D., van den Broeke, M., Reijmer, C. and van de Wal, R.: The summer surface energy balance of the high Antarctic plateau, Boundary-Layer Meteorol., 115(2), 289–317, https://doi.org/10.1007/s10546-004-4631-1, 2005.

van As, D., Box, J. E. and Fausto, R. S.: Challenges of quantifying meltwater retention in snow and firn: An expert elicitation, Front. Earth Sci., 4(November), 1–5, https://doi.org/10.3389/feart.2016.00101, 2016.

Van Den Broeke, M. R., Enderlin, E. M., Howat, I. M., Kuipers Munneke, P., Noël, B. P. Y., Jan Van De Berg, W., Van

700   Meijgaard, E. and Wouters, B.: On the recent contribution of the Greenland ice sheet to sea level change, Cryosphere, 10(5), 1933–1946, https://doi.org/10.5194/tc-10-1933-2016, 2016.

Van Genuchten, M. T.: Closed-Form Equation for Predicting the Hydraulic Conductivity of Unsaturated Soils., Soil Sci. Soc. Am. J., 44(5), 892–898, https://doi.org/10.2136/sssaj1980.03615995004400050002x, 1980.

Van Kampenhout, L., Lenaerts, J. T. M., Lipscomb, W. H., Sacks, W. J., Lawrence, D. M., Slater, A. G. and van den Broeke,

705   M. R.: Improving the Representation of Polar Snow and Firn in the Community Earth System Model, J. Adv. Model. Earth Syst., 9(7), 2583–2600, https://doi.org/10.1002/2017MS000988, 2017.

Van Pelt, W. J. J., Oerlemans, J., Reijmer, C. H., Pohjola, V. A., Pettersson, R. and Van Angelen, J. H.: Simulating melt, runoff and refreezing on Nordenskiöldbreen, Svalbard, using a coupled snow and energy balance model, Cryosphere, 6(3), 641–659, https://doi.org/10.5194/tc-6-641-2012, 2012.

710   Van Pelt, W., Pohjola, V., Pettersson, R., Marchenko, S., Kohler, J., Luks, B., Ove Hagen, J., Schuler, T. V., Dunse, T., Noël, B. and Reijmer, C.: A long-term dataset of climatic mass balance, snow conditions, and runoff in Svalbard (1957-2018), Cryosphere, 13(9), 2259–2280, https://doi.org/10.5194/tc-13-2259-2019, 2019.

Vandecrux, B., Fausto, R. S., Langen, P. L., van As, D., MacFerrin, M., Colgan, W. T., Ingeman-Nielsen, T., Steffen, K., Jensen, N. S., Møller, M. T. and Box, J. E.: Drivers of Firn Density on the Greenland Ice Sheet Revealed by Weather Station

715   Observations and Modeling, J. Geophys. Res. Earth Surf., 123(10), 2563–2576, https://doi.org/10.1029/2017JF004597, 2018.

Vandecrux, B., MacFerrin, M., MacHguth, H., Colgan, W. T., Van As, D., Heilig, A., Max Stevens, C., Charalampidis, C., Fausto, R. S., Morris, E. M., Mosley-Thompson, E., Koenig, L., Montgomery, L. N., Miège, C., Simonsen, S. B., Ingeman-

Nielsen, T. and Box, J. E.: Firn data compilation reveals widespread decrease of firn air content in western Greenland, Cryosphere, 13(3), 845–859, https://doi.org/10.5194/tc-13-845-2019, 2019.

720   Verjans, V., Leeson, A. A., Max Stevens, C., MacFerrin, M., Noël, B. and Van Den Broeke, M. R.: Development of physically based liquid water schemes for Greenland firn-densification models, Cryosphere, 13(7), 1819–1842, https://doi.org/10.5194/tc-13-1819-2019, 2019.

Vionnet, V., Brun, E., Morin, S., Boone, A., Faroux, S., Le Moigne, P., Martin, E. and Willemet, J. M.: The detailed snowpack scheme Crocus and its implementation in SURFEX v7.2, Geosci. Model Dev., 5(3), 773–791, https://doi.org/10.5194/gmd-725   5-773-2012, 2012.

Wever, N., Fierz, C., Mitterer, C., Hirashima, H. and Lehning, M.: Solving Richards Equation for snow improves snowpack meltwater runoff estimations in detailed multi-layer snowpack model, Cryosphere, 8(1), 257–274, https://doi.org/10.5194/tc-8-257-2014, 2014.

Wever, N., Würzer, S., Fierz, C. and Lehning, M.: Simulating ice layer formation under the presence of preferential flow in 730   layered snowpacks, Cryosphere, 10(6), 2731–2744, https://doi.org/10.5194/tc-10-2731-2016, 2016.

Yamaguchi, S., Katsushima, T., Sato, A. and Kumakura, T.: Water retention curve of snow with different grain sizes, Cold Reg. Sci. Technol., 64(2), 87–93, https://doi.org/10.1016/j.coldregions.2010.05.008, 2010.

Zuo, Z. and Oerlemans, J.: Modelling albedo and specific balance of the Greenland ice sheet: Calculations for the Søndre Stromfjord transect, J. Glaciol., 42(141), 305–316, https://doi.org/10.3189/s0022143000004160, 1996.